

## Membrane-integrated microfluidic device for high-resolution live cell imaging

Alla A. Epshteyn,<sup>1</sup> Steven Maher,<sup>1,2</sup> Amy J. Taylor,<sup>1</sup> Angela B. Holton,<sup>1</sup> Jeffrey T. Borenstein,<sup>3</sup> and Joseph D. Cuiffi<sup>1</sup>

<sup>1</sup>Bioengineering Center, Charles Stark Draper Laboratory, Tampa, Florida 33612, USA

<sup>2</sup>College of Public Health, University of South Florida, Tampa, Florida 33612, USA

<sup>3</sup>Charles Stark Draper Laboratory, Department of Bioengineering, Cambridge, Massachusetts 02139, USA

(Received 31 May 2011; accepted 20 September 2011; published online 17 October 2011)

The design and fabrication of a membrane-integrated microfluidic cell culture device (five layers,  $\leq 500 \mu\text{m}$  total thickness) developed for high resolution microscopy is reported here. The multi-layer device was constructed to enable membrane separated cell culture for tissue mimetic *in vitro* model applications and pharmacodynamic evaluation studies. The microdevice was developed via a unique combination of low profile fluidic interconnect design, substrate transfer methodology, and wet silane bonding. To demonstrate the unique high resolution imaging capability of this device, we used oil immersion microscopy to image stained nuclei and mitochondria in primary hepatocytes adhered to the incorporated membrane © 2011 American Institute of Physics. [doi:10.1063/1.3647824]

### I. INTRODUCTION

Membrane-integrated cell culture inserts enable cell growth in adjacent chambers to create distinct environmental conditions but lack greater control over cellular microenvironment including dynamic flow conditions useful for pharmacodynamic research. The primary technique to model tissue mimetic biological interfaces is to utilize membrane inserts (such as Millicell<sup>TM</sup>, Transwell<sup>TM</sup>) that support co-culture of cells on opposite sides of the barrier. However, physiologically realistic *in vitro* models require greater control of the cellular microenvironment,<sup>1,2</sup> including dynamic flow conditions. The advent of microfluidic-based cell culture systems have overcome limitations in perfusion and are well-suited for multiplexed *in vitro* models.<sup>3</sup> Several microfluidic approaches that utilize either horizontally integrated membrane layers<sup>4-13</sup> or vertically defined features to create a biological barrier<sup>14</sup> have been reported. Such microfluidic cellular constructs have been seeded with different cell types on opposite sides of the membrane to demonstrate models of the alveolar-capillary interface,<sup>10</sup> smooth muscle cell-endothelial interface,<sup>6</sup> and endothelial cell-astrocytic end feet interface.<sup>7</sup> Furthermore, microfluidic constructs with cells seeded on only one side of the membrane have been used to evaluate endothelial layer integrity,<sup>11</sup> protect shear sensitive hepatocytes from perfusion,<sup>4</sup> and optimize perfusion conditions for renal tubular cells.<sup>12</sup>

While continuously perfused membrane integrated microfluidic devices have been developed for cell culture interface studies, the current technology lacks the ability to examine the cell culture on both sides of the membrane under oil immersion microscopy, a capability required for high content drug screening. Technical advances in high content screening have enabled the practical implementation of high throughput sub-cellular, high resolution imaging,<sup>15</sup> yet these data are not available when complex culture systems are optically inaccessible.

In this report, we present a novel microfluidic cell culture device which addresses the need for high resolution microscopy of a continuously perfused cell culture system on either side of a horizontally integrated membrane. To overcome fabrication challenges associated with membrane integration and the capability to perform high resolution microscopy, a substrate transfer technique was developed to allow non-free standing polymer thin-films to be transported

without any pattern stretching using an oxygen plasma treated carrier material. In addition, we modified a previously reported wet silane bonding technique<sup>16</sup> to accommodate the unique geometries of each thin film material layer. Finally, novel low profile fluidic ports and a device frame were developed to allow oil immersion objective access to the active area of the device needed for high resolution microscopy. To demonstrate live high resolution imaging capability within the device, we cultured hepatocytes on both sides of the membrane and used oil immersion microscopy to show subcellular structures.

## II. RESULTS AND DISCUSSION

Design criteria for the microfluidic device included (1) selective cell seeding on both sides of the membrane, (2) continuous nutrient perfusion, and (3) high resolution imaging access to both sides of the membrane. To meet these criteria, we selected materials, designed device geometry and fluidic interconnect constrained by oil immersion objective access, and developed subsequent device fabrication and assembly processes. The device consisted of 4 layers: a glass cover slip at the bottom, an intermediate Polydimethylsiloxane (PDMS) layer, a polycarbonate (PC) membrane, and PDMS layer on top as shown in (Fig. 1(a)). PDMS was chosen for its biocompatibility,<sup>17</sup> optical clarity, and ease of fabrication. The cover slip on the bottom allowed for high resolution microscopy and provided mechanical stability, while the thin PDMS layers facilitated higher gas exchange and also allowed for high resolution imaging on the other side of the membrane (Figs. 1(a)–1(c)). Based on prior work,<sup>18</sup> a track-etched PC membrane (10  $\mu\text{m}$  thick, 10  $\mu\text{m}$  pores) was incorporated into the device to tailor the surface chemistry for cell culture.

In addition to selecting suitable materials for the device fabrication and cell culture, the design criteria focused on the ability to perform high resolution microscopy. The working distance of an oil immersion 100 $\times$  objective is  $< \sim 300 \mu\text{m}$ , which constrains the distance between the objective and the cells on the membrane surface. A No. 1 glass coverslip is approximately 130  $\mu\text{m}$  thick, so the device was designed with a 100  $\mu\text{m}$  thick PDMS gasket, defining the perfusion cell chamber, between the coverslip and the bottom side of the membrane (Fig. 1(c)). The combination of the coverslip and PDMS gasket thinness (230  $\mu\text{m}$  total) ensured that the membrane was within the objective working distance. On the opposite side of the membrane,

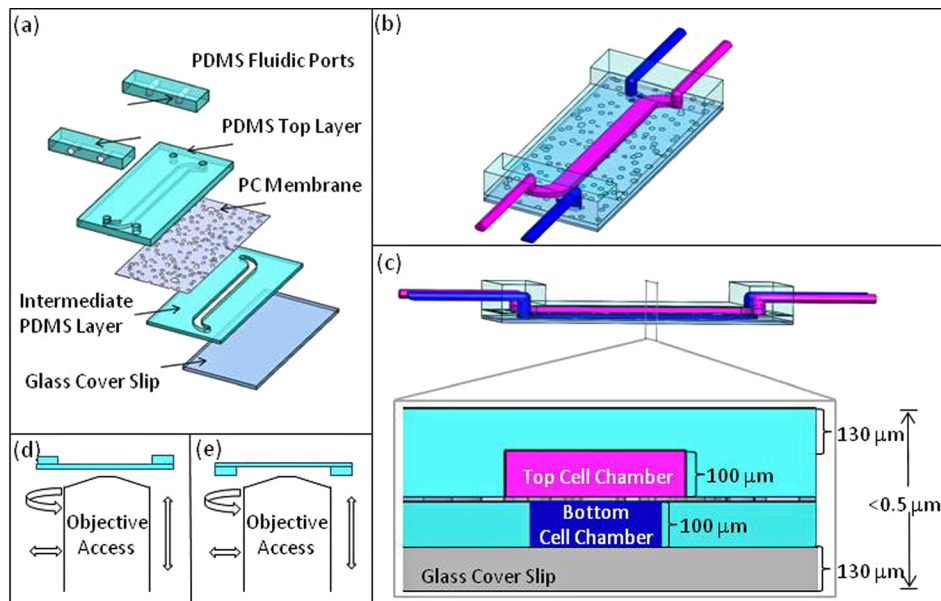


FIG. 1. (a) An illustration of device components. (b) Device concept with represented top (magenta) and bottom (blue) chamber flows. (c) Expanded cross-sectional view of device with cell chamber dimensions optimized for high-resolution oil immersion microscopy. (d) and (e) Low profile fluidic ports allow for optical access to top and bottom membrane cell culture chambers.

instead of a glass coverslip and PDMS gasket, one PDMS layer defined both the cell chamber and the upper support material. The distance from objective to membrane was designed to be equal (also  $230\ \mu\text{m}$  total) from both sides of the membrane (Fig. 1(c)). The layout of the device was designed with channel widths based on prior work<sup>4</sup> and a channel length of 34 mm. Each chip was designed with two independent devices on a glass cover slip to demonstrate the potential for fabricating an array of cell chambers for applications in high through put studies.

PDMS thin-films are prone to wrinkling and are difficult to handle. Consequently, the molded PDMS thin-film needed to be transferred onto a carrier material during assembly. We developed a novel technique that enables the transfer of a PDMS thin-film from the wafer to a Kapton<sup>TM</sup> film without creating any feature distortion that is often observed due to the PDMS stretching (Fig. 2(a)). In this technique, Kapton is oxygen plasma treated before it is placed on top of uncured PDMS in a load chamber. Upon PDMS curing, the PDMS film formed a temporary bond to the Kapton film, resulting in no PDMS thin-film distortion (Fig. 2(b)). A similar substrate transfer method was previously reported<sup>19</sup> utilizing PDMS as a carrier material, instead of Kapton. As a carrier material, Kapton provided a clear interface distinction between the carrier material and patterned PDMS, and Kapton had transparent properties which are advantageous for thin film alignment during assembly. In addition, as a thermoset, Kapton withstood high mechanical loads useful for creating punched through patterned PDMS thin-films. In sum, Kapton provided temporary bonding, transparency, material distinction, and high temperature and pressure tolerance, all necessary for fabrication and transfer of PDMS thin-films.

Following substrate transfer, the PC membrane was sandwiched between the top layer and the intermediate PDMS layers (Figs. 3(a) and 3(b)) using wet silane (3-aminopropyltriethoxysilane–APTES) chemistry with modifications from prior work.<sup>16</sup> Aran *et al.* reported that oxygen plasma treating PC and PDMS surfaces followed by a wet APTES treatment of the PC resulted in an irreversible bond between the two when mated and heated. We were able to bond untreated PC membranes to PDMS that received APTES treatment after oxygen plasma. In addition, the bonding protocol was modified from a single temperature cure to incremental heating steps to reduce bonding defects such as bubbles in the membrane and PDMS interfaces. In order to prevent wrinkling and tearing of the thin membranes, critical care was required during device fabrication. The membrane was placed on a quartz plate and secured with glass slides during plasma treatment. During APTES bonding, the membranes were carefully lifted by soft tipped tweezers over PDMS and allowed to settle into the bonding position.

Tubing connections to the thin device ( $<500\ \mu\text{m}$ ) required additional fluidic port development. The fluidic ports were fabricated using PDMS to avoid the introduction of a new material for cell culture. The fluidic ports were aligned and bonded to the channel entry points of the chip (Fig. 3(d)). In addition to fluidic ports, a rapid prototyped frame was designed to secure the chip and tubing specifically for inverting the chip during microscopy. The key feature of both the frame and the fluidic ports was their low profile design necessary to accommodate lateral movement of objective lenses (Figs. 1(d) and 1(e)). The combination of fluidic port design

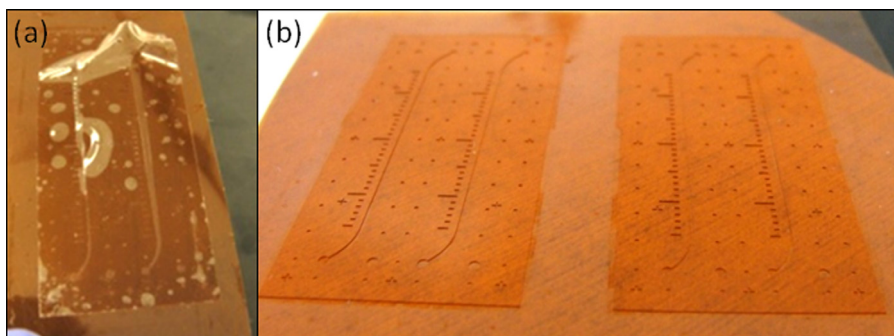


FIG. 2. (a) Thin polymer films can be stretched and deformed when peeled from a wafer. (b) The structure of a polymer thin-film was retained during transfer. This was achieved by surface treating the carrier material, resulting in a temporary bond to the polymer film.

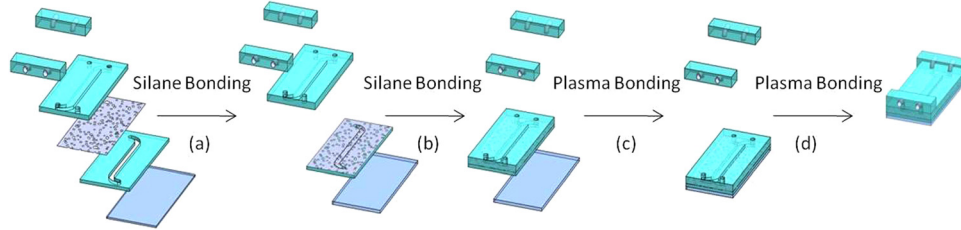


FIG. 3. Step-by-step assembly overview of device fabrication. The PC membrane was bonded first to the intermediate PDMS layer on one side (a), then to top PDMS layer on the other side (b) via silane chemistry. Plasma bonding was utilized to bond the glass coverslip to stack (c) as well as the manifolds to device (d).

and frame allowed for high-resolution imaging access to live cell culture on both sides of the membrane and the entire set up on a microscope stage is shown in Figure 4.

To demonstrate the imaging capabilities of the device, primary hepatocytes were stained and then seeded into the device. In one device, cells were seeded on top of the membrane and perfused through the bottom chamber. In a second device, cells were seeded on the bottom of the membrane and perfused through the top chamber. Intact DNA nuclear content and cytoplasmic individual mitochondria were successfully captured through fluorescent imaging within hepatocytes captured in real-time, while the device was under perfusion, demonstrating the efficacy of the device to afford oil immersion microscopy on both sides of the membrane (Fig. 5).

While oil immersion imaging capabilities on both sides of the membrane in the device were demonstrated, further evaluation studies will be executed in future work to validate long term cell culture viability in the device. However, in previous work,<sup>4</sup> viable cell culture has been sustained in a similar membrane-integrated dual cell chamber system for weeks supporting the viability hypothesis of our device. In addition, the effective membrane permeability has been modeled for dual chamber device<sup>20</sup> in a similar configuration and a similar membrane. The model predicted sufficient oxygen concentrations for cells in the lower chamber, suggesting sufficient oxygen gas transfer in this device.

### III. EXPERIMENTAL

The device was composed of glass cover slip (No. 1), a PC membrane (1215043, GE Osmonics, Trevose, PA), 2 PDMS (Dow Sylgard 184, Midland, MI) chamber layers molded from custom-patterned SU-8 (Microchem Co, Newton, MA) silicon wafers, and PDMS fluidic ports. The wafers were vapor deposited with (Tridecafluoro-1,1,2,2-tetrahydrooctyl) trichlorosilane (Gelest Inc, Morrisville, PA) for ease of PDMS removal. An SU-8 wafer mold was used to pattern the top PDMS layer (Fig. 1(d)) by spinning two layers of uncured PDMS (10:1 polymer base to curing agent) to a final thickness of  $230\ \mu\text{m}$  at 650 rpm for 60 s. We found that to achieve a  $230\ \mu\text{m}$  thickness, a 2 step spinning process produced a significantly more uniform film thickness than a single spin. The intermediate PDMS layer (Fig. 1(d)) with through-hole features was fabricated by curing PDMS using a previously described custom lamination

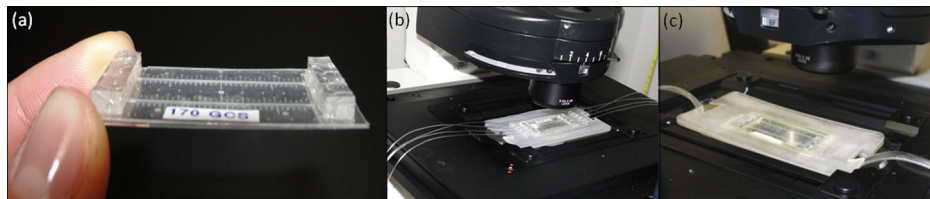


FIG. 4. (a) Two fully fabricated devices on one glass chip illustrate the potential for high throughput. (b) A multilayer device in a robust custom built frame with tubing connected to fluidic ports; fits a Leica microscope holder without hindering any lateral objective movement. (c) The entire chip-in-frame system can be flipped over for oil immersion microscopy access to the opposite side of the membrane side.

chamber at 40 psi at 65 °C for 25 min.<sup>21</sup> Fluidic ports were punched in a PDMS block with a 1.5 mm biopsy punch.

To transfer the intermediate PDMS layer from the patterned wafer, HN grade Kapton (DuPont Electronics, Wilmington, DE) was oxygen plasma treated (Harrick, 300 mTorr, 2 min, 30 W) before placing on top of the uncured PDMS in the lamination chamber. The laminated PDMS layer, still on the Kapton substrate, was plasma treated (300 mTorr, 2 min, 30 W) and then soaked in an APTES/Deionized water solution (5%v/v) for 20 min at 80 °C. This APTES treated PDMS layer was then bonded to an untreated PC membrane by heating at 37 °C for 5 min. The same APTES solvent treatment was used to bond the aligned PDMS top layer to the exposed PC surface of the stack (Figs. 3(a) and 3(b)). This bond was cured at room temperature for 1–3 h followed by 3–8 h at 37 °C and 1–3 h at 65 °C. The Kapton was released from the laminated PDMS layer by the spraying isopropanol at the interface of Kapton and laminated PDMS. A No. 1 glass cover slip and low profile fluidic ports (1.5 mm diameter biopsy punched) were bonded to the laminated PDMS layer surface of the stack via described plasma treatment (Figs. 3(c) and 3(d)). Finally, the SolidWorks designed frame was fabricated using a Stratasys FDM 3D printer.

After the devices were fabricated, the PC membranes were coated with collagen by flowing a collagen solution (0.067 mg/ml in 0.02 N acetic acid) through the cell chambers. This, along with the plasma treatment of PC membrane during device assembly, increased the hydrophilicity of the PC membrane as well as prepared the channels for cell seeding. After this treatment, no issues in wetting the membrane or flowing media through the pores were observed.

The primary hepatocytes (Sciencell, Carlsbad, CA and Lonza, Walkersville, MD) mitochondria and nuclei were stained with 500 nM of Mitotracker<sup>TM</sup> Red (Invitrogen, Carlsbad, CA) and 10 ng/ml of Hoechst 33342 (Sigma, St. Louis, MO) diluted in PBS. After 1 h of stain and subsequent washing with PBS, cells were trypsinized, loaded into a syringe and slowly perfused into either the top or the bottom channel. Cells were given 6 h to attach to the collagen coated membrane, while the opposite channel was under media perfusion at 90  $\mu$ l/h. Subcellular

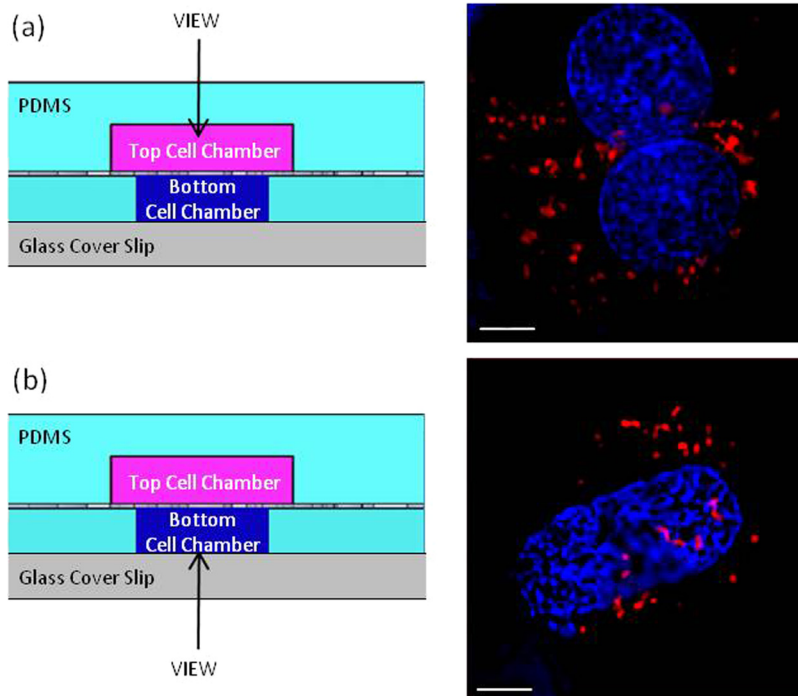


FIG. 5. (a) Primary hepatocytes in top channel observed through PDMS layer identifying mitochondria (red) and nuclei (blue). (b) Primary hepatocytes in bottom channel observed through cover glass identifying mitochondria (red) and nuclei (blue). Magnified by an oil immersion 100 $\times$  objective; 5  $\mu$ m scale bar.

content was imaged with a 100 × oil immersion objective on a Deltavision Core (Applied Precision, Issaquah, WA).

#### IV. CONCLUSIONS

We successfully designed and fabricated a membrane-integrated microfluidic device for perfused multi-compartment cell culture amenable for high resolution imaging. The thin device design with compact fluidic ports and frame allowed for oil immersion live cell imaging on either side of the internal membrane. Future work will focus on validating the device platform for long term viable cell culture. And then move towards high throughput design and automation of the device fabrication and assembly. Such a high throughput design will provide a platform for a continuously perfused pharmaceutical evaluation system in real-time with high resolution (e.g., oil immersion) visualization of subcellular pharmacodynamics.

#### ACKNOWLEDGMENTS

This work was supported by Draper internal funding and by the State of Florida. The authors thank James Hsiao for guidance on device design, Dr. Anil Kumar H. Achyuta for manuscript editing, and Dr. John Adams (University of South Florida) for access to the Deltavision microscope.

- <sup>1</sup>L. G. Griffith and M. A. Swartz, *Nat. Rev. Mol. Cell. Biol.* 7(3), 211 (2006).
- <sup>2</sup>A. Khademhosseini, R. Langer, J. Borenstein, and J. P. Vacanti, *Proc. Natl. Acad. Sci. U.S.A* 103(8), 2480 (2006).
- <sup>3</sup>M. H. Wu, S. B. Huang and G. B. Lee, *Lab Chip* 10(8), 939 (2010).
- <sup>4</sup>A. Carraro, W. M. Hsu, K. M. Kulig, W. S. Cheung, M. L. Miller, E. J. Weinberg, E. F. Swart, M. Kaazempur-Mofrad, J. T. Borenstein, J. P. Vacanti, and C. Neville, *Biomed. Microdevices* 10(6), 795 (2008).
- <sup>5</sup>D. M. Cate, C.G. Sip, and A. Folcha, *Biomicrofluidics* 4, 044405 (2010).
- <sup>6</sup>S. Duncanson, T. Kniazeva, M. E. Keegan, E. B. Finkelstein, G. E. Owens, R. Soong, J. Hsiao, K. Y. Eng, L. Pomerantseva, C. M. Neville, D. M. Hoganson, J. P. Vacani, J. R. Turk, and J. T. Borenstein, in TEMIS - NA 2008 Conference & Expo (San Diego, CA, 2008).
- <sup>7</sup>S. H. Ma, L. A. Lepak, R. J. Hussain, W. Shain, and M. L. Shuler, *Lab Chip* 5(1), 74 (2005).
- <sup>8</sup>J. W. Song, S. P. Cavnar, A. C. Walker, K. E. Luker, M. Gupta, Y. C. Tung, G. D. Luker, and S. Takayama, *PLoS One* 4(6), e5756 (2009).
- <sup>9</sup>D. Huh, H. Fujioka, Y. C. Tung, N. Futai, R. Paine, 3rd, J. B. Grobberg, and S. Takayama, *Proc. Natl. Acad. Sci. U.S.A* 104(48), 18886 (2007).
- <sup>10</sup>D. Huh, B. D. Matthews, A. Mammoto, M. Montoya-Zavala, H. Y. Hsin, and D. E. Ingber, *Science* 328(5986), 1662 (2010).
- <sup>11</sup>J. Shao, L. Wu, J. Wu, Y. Zheng, H. Zhao, X. Lou, Q. Jin, and J. Zhao, *Biomed Microdevices* 12(1), 81 (2010).
- <sup>12</sup>K. J. Jang and K. Y. Suh, *Lab Chip* 10(1), 36 (2010).
- <sup>13</sup>S. Sriganapalan, C. Lam, A. R. Wheeler, and C. A. Simmons, *Biomicrofluidics* 5(1), 13409 (2011).
- <sup>14</sup>P. J. Lee, P. J. Hung, and L. P. Lee, *Biotechnol. Bioeng.* 97(5), 1340 (2007).
- <sup>15</sup>F. Zanella, J. B. Lorens, and W. Link, *Trends Biotechnol.* 28(5), 237 (2010).
- <sup>16</sup>K. Aran, L. A. Sasso, N. Kamdar, and J. D. Zahn, *Lab Chip* 10(5), 548 (2010).
- <sup>17</sup>D. Wlodkowic, S. Faley, J. Skommer, D. McGuinness, and J. M. Cooper, *Anal. Chem.* 81(23), 9828 (2009).
- <sup>18</sup>J. T. Borenstein, *MRS Proceedings* 1139, (GG02-01) (2008).
- <sup>19</sup>M. Zhang, J. Wu, L. Wang, K. Xiao, and W. Wen, *Lab Chip* 10(9), 1199 (2010).
- <sup>20</sup>N. K. Inamdar, L. G. Griffith, and J. T. Borenstein, *Biomicrofluidics* 5, 022213 (2011).
- <sup>21</sup>C. W. Yung, J. Fiering, A. J. Mueller, and D. E. Ingber, *Lab Chip* 9(9), 1171 (2009).